iScience, Volume *27*

Supplemental information

Opportunistic pathogen *Porphyromonas gingivalis* targets the LC3B-ceramide complex and mediates lethal mitophagy resistance in oral tumors

Megan Sheridan, Nityananda Chowdhury, Bridgette Wellslager, Natalia Oleinik, Mohamed Faisal Kassir, Han G. Lee, Mindy Engevik, Yuri Peterson, Subramanya Pandruvada, Zdzislaw M. Szulc, Özlem Yilmaz, and Besim Ogretmen

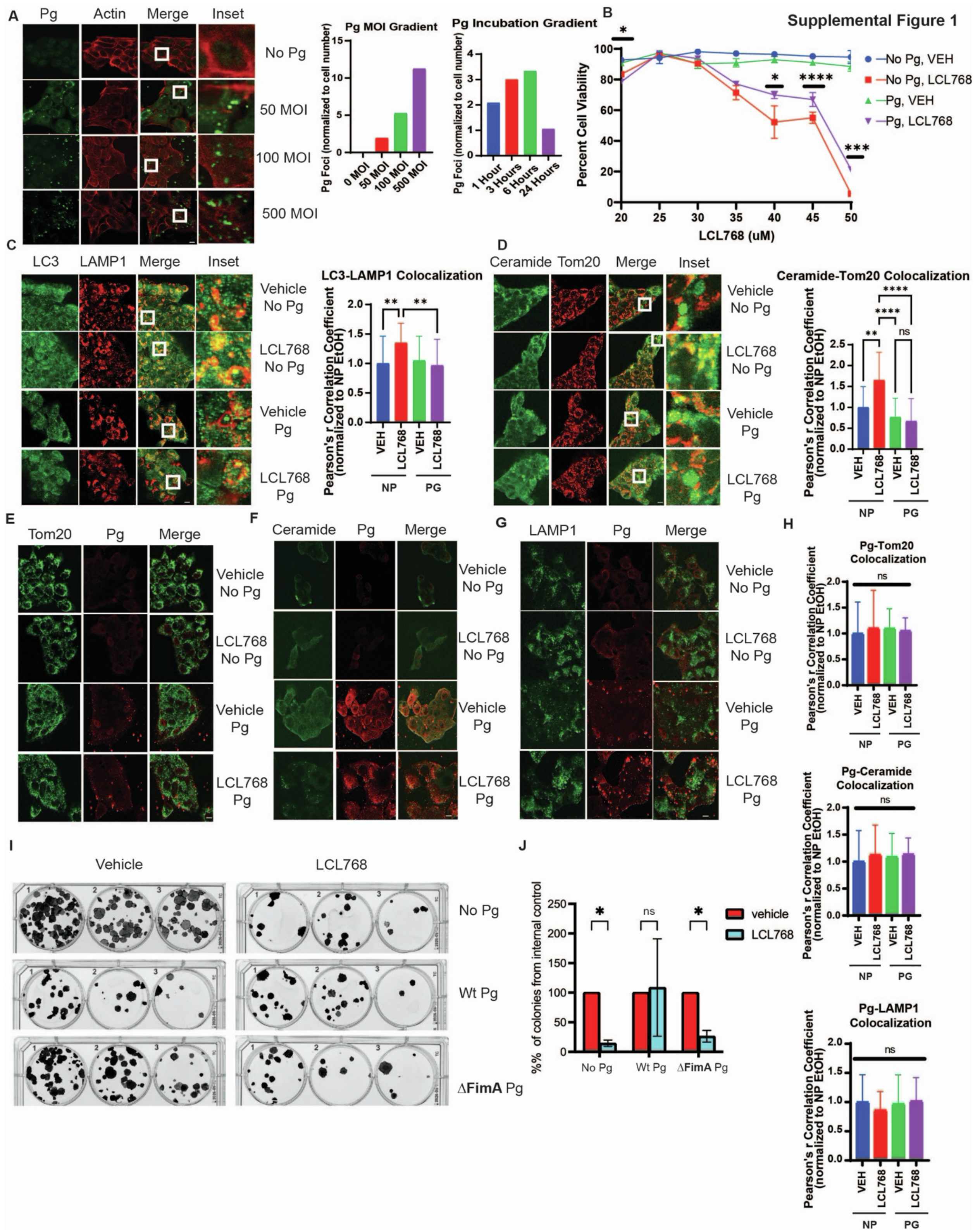
Supplemental Figure 1
A
Pg
Actin
Merge
Inset
No Pg
50 MOI
100 MOI
500 MOI
Pg MOI Gradient
Pg Foci (normalized to cell number)
0 MOI
50 MOI
100 MOI
500 MOI
Pg Incubation Gradient
1 Hour
3 Hours
6 Hours
24 Hours
B
Percent Cell Viability
LCL768 (uM)
No Pg, VEH
No Pg, LCL768
Pg, VEH
Pg, LCL768
C
LC3
LAMP1
Merge
Inset
Vehicle No Pg
LCL768 No Pg
Vehicle Pg
LCL768 Pg
LC3-LAMP1 Colocalization
Pearson's r Correlation Coefficient (normalized to NP EtOH)
VEH
LCL768
NP
PG
D
Ceramide
Tom20
Merge
Inset
Ceramide-Tom20 Colocalization
E
Tom20
Pg
Merge
F
Ceramide
Pg
Merge
G
LAMP1
Pg
Merge
H
Pg-Tom20 Colocalization
Pg-Ceramide Colocalization
Pg-LAMP1 Colocalization
ns
I
Vehicle
LCL768
No Pg
Wt Pg
ΔFimA Pg
J
%% of colonies from internal control
vehicle
LCL768
No Pg
Wt Pg
ΔFimA Pg

Supplemental Figure S1. Analysis of additional mitophagy markers and their association with *P. gingivalis,* Related to Figure 1. A. Confocal images of *P. gingivalis* (green) internalization into UMSCC1A cells labeled with actin antibody (red) at increasing multiplicity of infection (MOI) or incubation time (hr) for the purpose of infection optimization. The bottom panels show the quantification of intracellular *P. gingivalis* foci normalized to cell number in confocal images using ImageJ Fiji software for both multiplicity of infection (MOI) and incubation optimization. **B.** Live UMSCC1A cells infected or uninfected with *P. gingivalis* were treated with increasing concentrations of LCL768 or vehicle control for 2 hours and stained with trypan blue cell exclusion dye. Cell viability (percent live, unstained cells) is shown as means ± SD (n=3, *P<0.05, ***P<0.001, ****P<0.0001). **C.** Confocal microscopy of UMSCC1A cells infected/uninfected with *P. gingivalis* (100 MOI, 6 hours) and treated with vehicle or LCL768 (30 μM, 2 hours) were labeled with LC3 (green) and LAMP1 (red) antibodies. Yellow shows colocalization. Images represent three independent experiments. **D.** Confocal images of ceramide (green) and Tom20 (red) are shown. Colocalization in confocal images was quantified, shown via Pearson's correlation coefficient in the panel below, and normalized to uninfected, untreated control. Values indicate mean ± SD of n=3 independent experiments. Ns, not significant, **P<0.01, ****P<0.0001. **E-G.** Confocal microscopy of antibody-labeled *P. gingivalis* association with Tom20, ceramide, and LAMP1 in UMSCC1A cells infected/uninfected with *P. gingivalis* (100 MOI) for 6 hours and treated/not treated with 30 μM LCL768 for 2 hours. **H.** Quantification of colocalization was estimated via Pearson's correlation coefficient, completed with ImageJ Fiji software, and normalized to uninfected, untreated control. Values indicate mean ± SD of n=3 independent experiments. Ns, not significant. **I-J.** Clonogenic assay of UMSCC1A cells infected/uninfected with wildtype or ΔFimA *P. gingivalis* (100 MOI, 6 hr) and

treated/untreated with 15 μM LCL768 for 3 hours as a pretreatment prior to preparation of single-cell suspensions. Single cells were seeded in 6-well plates and incubated for about two weeks until colonies were counted. Values indicate mean ± SD of n=3 independent experiments and were normalized to corresponding vehicle-treated cells.

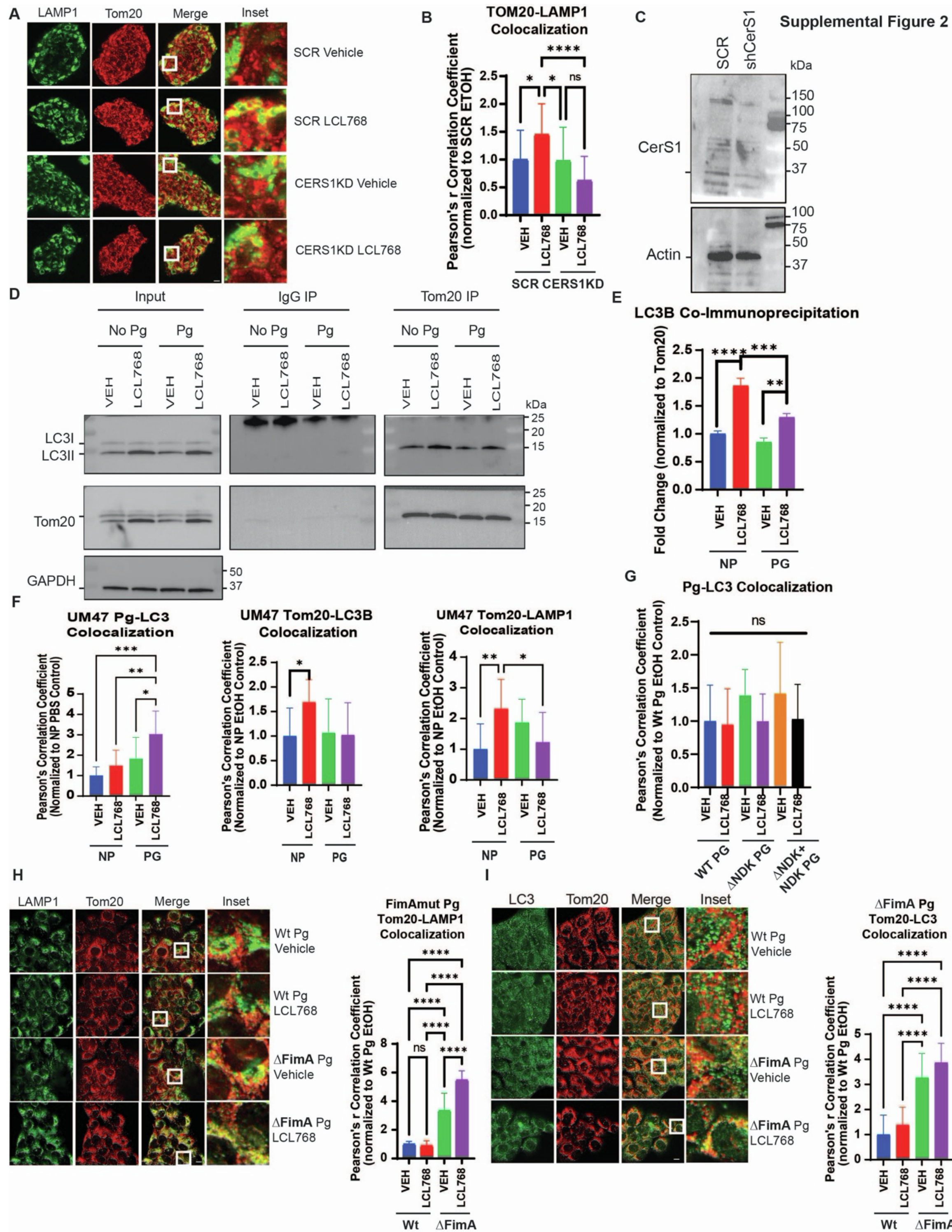
Supplemental Figure 2
A
LAMP1
Tom20
Merge
Inset
SCR Vehicle
SCR LCL768
CERS1KD Vehicle
CERS1KD LCL768
B
TOM20-LAMP1 Colocalization
Pearson's r Correlation Coefficient (normalized to SCR ETOH)
SCR CERS1KD
C
SCR
shCerS1
kDa
CerS1
Actin
D
Input
IgG IP
Tom20 IP
No Pg
Pg
VEH
LCL768
LC3I
LC3II
Tom20
GAPDH
E
LC3B Co-Immunoprecipitation
Fold Change (normalized to Tom20)
NP
PG
F
UM47 Pg-LC3 Colocalization
UM47 Tom20-LC3B Colocalization
UM47 Tom20-LAMP1 Colocalization
Pearson's Correlation Coefficient (Normalized to NP PBS Control)
Pearson's Correlation Coefficient (Normalized to NP EtOH Control)
G
Pg-LC3 Colocalization
Pearson's Correlation Coefficient (Normalized to Wt Pg EtOH Control)
WT PG
ΔNDK PG
ΔNDK+ NDK PG
H
Wt Pg Vehicle
Wt Pg LCL768
ΔFimA Pg Vehicle
ΔFimA Pg LCL768
FimAmut Pg Tom20-LAMP1 Colocalization
Pearson's r Correlation Coefficient (normalized to Wt Pg EtOH)
Wt
ΔFimA
I
LC3
ΔFimA Pg Tom20-LC3 Colocalization

Supplemental Figure S2. Mitophagy inhibition in HPV- and HPV+ oral squamous cell carcinoma expressing ceramide synthase 1 (CerS1) knockdown or infection with *P. gingivalis* and its isogenic mutant strains, Related to Figure 1. A. Confocal images of UMSCC1A cells stably expressing shRNA against CerS1 and treated with vehicle or LCL768 were dual labeled for LAMP1 (green) and Tom20 (red). Yellow shows colocalization. Images represent three independent experiments. **B.** Quantification of images in (**A**). Pearson's correlation coefficient was normalized to scrambled shRNA, untreated control. Data are means ± SD (n=3, ns, not significant, *P<0.05, ****P<0.0001). **C.** Western blotting was completed to determine protein abundance of stably knocked down CerS1 in UMSCC1A cells. Actin was used as the loading control. **D.** UMSCC1A cells were infected/uninfected with *P. gingivalis* (100 MOI, 6 hours), treated with vehicle or LCL768 (30 μM, 2 hours), and lysed for immunoprecipitation with either Tom20 antibody (right) or species-matched IgG control antibody (middle). Co-immunoprecipitation for LC3B was resolved via western blotting. Input controls (pre-immunoprecipitation, left) were normalized to GAPDH. Images represent at least three independent experiments. **E.** Quantification of co-immunoprecipitated LC3B western blot bands in (**D**) normalized to scrambled shRNA, untreated control. Data are means ± SD (n=3, **P<0.01, ***P<0.001). **F.** UMSCC47, an HPV16+ oral squamous cell carcinoma line, was infected with *P. gingivalis* (100 MOI, 6 hours) and treated with LCL768 or vehicle (2 hours). Cells were dual labeled with *P. gingivalis* and LC3, Tom20 and LC3, or Tom20 and LAMP1 antibodies for confocal microscopy. Images represent at least three independent experiments. Quantification of colocalization was estimated via Pearson's correlation coefficient, completed with ImageJ Fiji software, and normalized to uninfected, untreated control. Values indicate mean ± SD of n=3 independent experiments. *P<0.05, **P<0.01, ***P<0.001. **G.** Additional *P. gingivalis* virulence

factors were analyzed for their effect on mitophagy induction by LCL768. Quantification of confocal images of UMSCC1A cells infected with wildtype (ATCC 33277), nucleoside-diphosphate-kinase (NDK) deficient mutant strain (ΔNDK), and the complemented NDK strain (ΔNDK+NDK) *P. gingivalis* (100 MOI, 6 hours) (5, 36). Quantification of colocalization was estimated via Pearson's correlation coefficient. Values indicate mean ± SD of n=3 independent experiments. Ns not significant, *P<0.05, **P<0.01, ***P<0.001, ****P<0.0001. **H, I.** UMSCC1A cells infected with wildtype (WT) or FimA mutant (ΔFimA) *P. gingivalis* and treated with LCL768 or vehicle control were dual labeled with LAMP1 (green) and Tom20 (red) or LC3 (green) and Tom20 (red) antibodies for confocal imaging. Yellow indicates colocalization. Quantification of colocalization was estimated via Pearson's correlation coefficient. Values indicate mean ± SD of n=3 independent experiments. Ns not significant, ****P<0.0001.

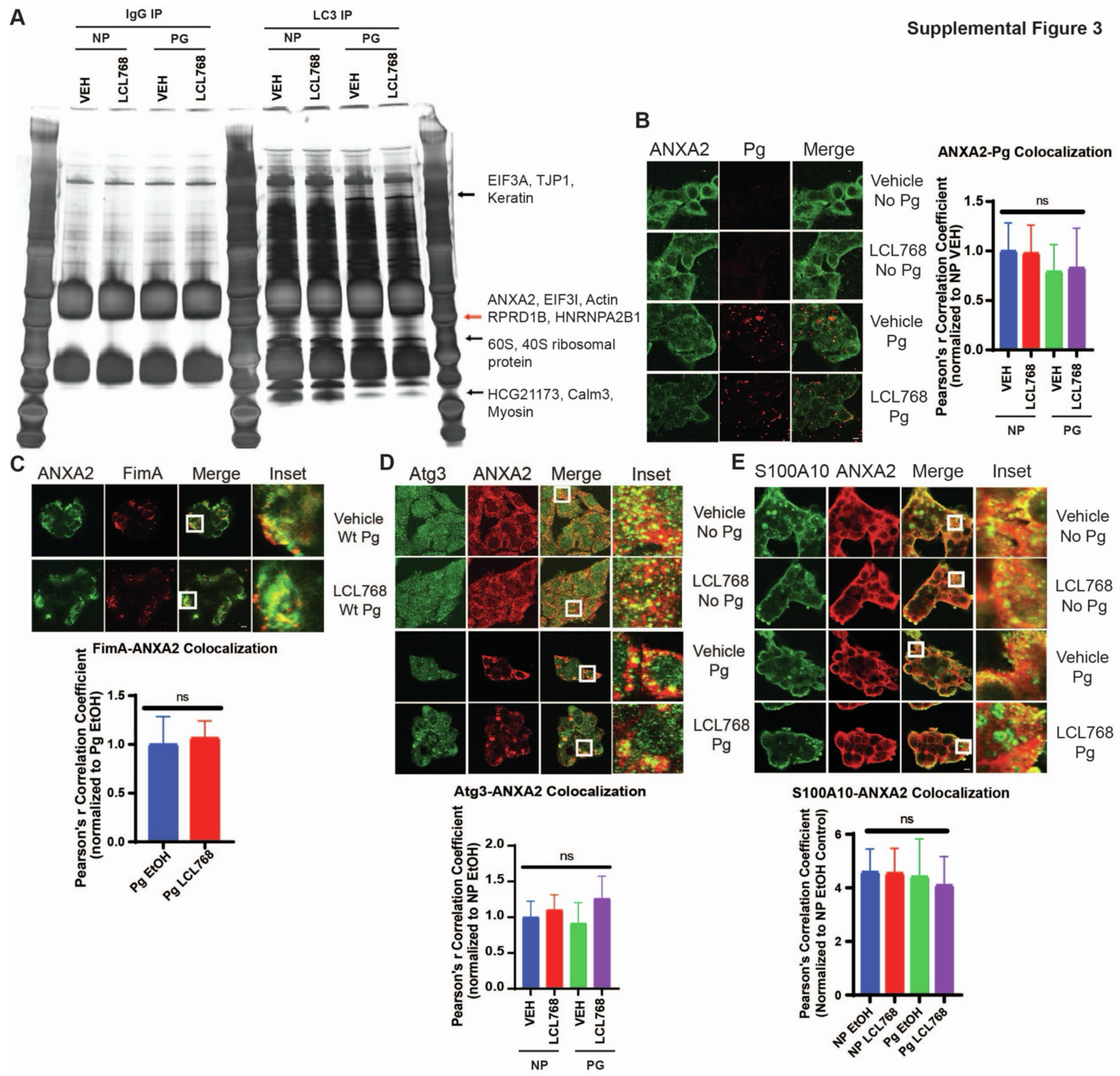
Supplemental Figure 3
A
IgG IP
LC3 IP
NP
PG
VEH
LCL768
EIF3A, TJP1, Keratin
ANXA2, EIF3I, Actin RPRD1B, HNRNPA2B1
60S, 40S ribosomal protein
HCG21173, Calm3, Myosin
B
ANXA2
Pg
Merge
Vehicle No Pg
LCL768 No Pg
Vehicle Pg
LCL768 Pg
ANXA2-Pg Colocalization
Pearson's r Correlation Coefficient (normalized to NP VEH)
ns
C
ANXA2
FimA
Merge
Inset
Vehicle Wt Pg
LCL768 Wt Pg
FimA-ANXA2 Colocalization
Pearson's r Correlation Coefficient (normalized to Pg EtOH)
Pg EtOH
Pg LCL768
D
Atg3
ANXA2
Merge
Inset
Atg3-ANXA2 Colocalization
Pearson's r Correlation Coefficient (normalized to NP EtOH)
E
S100A10
ANXA2
Merge
Inset
S100A10-ANXA2 Colocalization
Pearson's Correlation Coefficient (Normalized to NP EtOH Control)
NP EtOH
NP LCL768
Pg EtOH
Pg LCL768

Supplemental Figure S3. ***P. gingivalis*** **fimbriae A (FimA) associates with ANXA2, Related to Figure 2. A.** SDS-PAGE analysis of proteins bound to LC3 in UMSCC1A cells treated with LCL768. Binding to species-matched IgG antibodies was used as a control for nonspecific binding. Bands were visualized via silver stain, excised, and analyzed by mass spectrometry. The identified protein content for each submitted band is listed on the right. **B.** Confocal images of UMSCC1A cells infected/uninfected with *P. gingivalis* (100 MOI, 6 hours) and treated with vehicle or LCL768 (30 µM, 2 hours), dual-labeled with Annexin A2 (ANXA2, green) and *P. gingivalis* (red) antibodies. Images represent three independent experiments. Quantification of confocal images is shown via Pearson's correlation coefficient. Values indicate mean ± SD of n=3 independent experiments. Ns, not significant. **C.** UMSCC1A cells were infected with wildtype (ATCC 33277) *P. gingivalis* strain for 6 hours (100 MOI) before treatment with LCL768 or vehicle control (30 µM, 2 hours). Fimbriae A (FimA, red) association with ANXA2 (green) is shown via confocal microscopy using FimA *P. gingivalis* and ANXA2 antibodies. **D.** Confocal images of ANAX2 association with Atg3 in UMSCC1A cells infected/uninfected with *P. gingivalis* and treated with LCL768 or vehicle control. Pearson's correlation coefficient values indicate mean ± SD of n=3 independent experiments. "Ns" (not significant). **E.** Confocal images of S100A10 (p11, green) and ANXA2 (red) in UMSCC1A cells infected with *P. gingivalis* and treated with LCL768 are shown. Yellow shows colocalization. Images represent three independent experiments. Pearson's correlation coefficient values indicate mean ± SD of n=3 independent experiments. Ns not significant.

Supplemental Figure 4

A **FimA-LC3 Modelling**

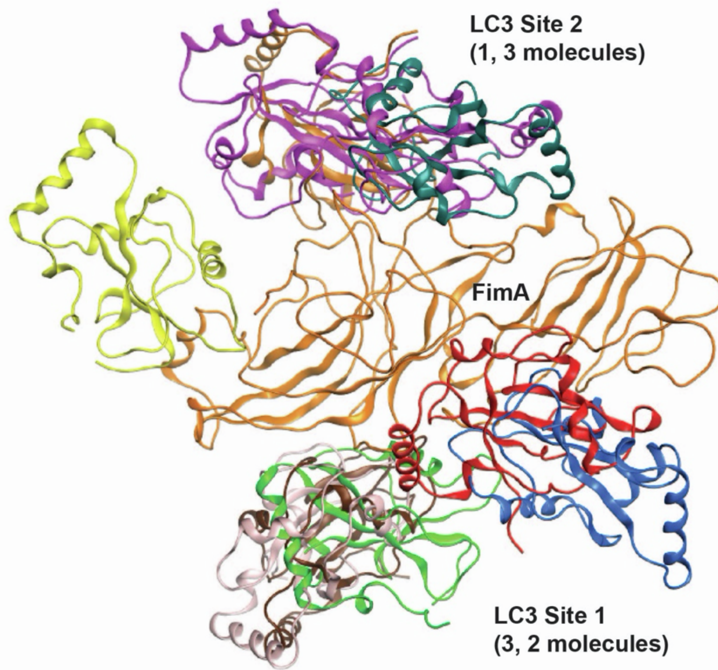

B **FimA-ANXA2 Modeling**

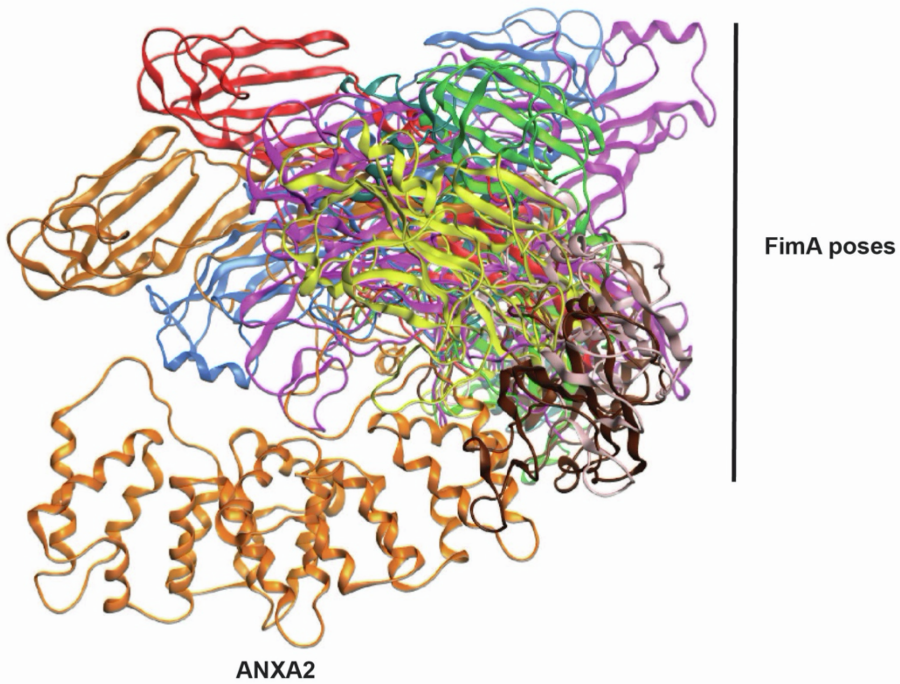

Supplemental Figure S4. Monomeric *P. gingivalis* FimA was projected with interact with ANXA2, not LC3, by *in silico* modelling, Related to Figure 4. A. Bimolecular modeling of FimA and LC3 showing little consensus in projected protein-protein interaction. **B.** Bimolecular modeling of FimA and ANXA2 showing protein docking.

Supplemental Figure 5

A

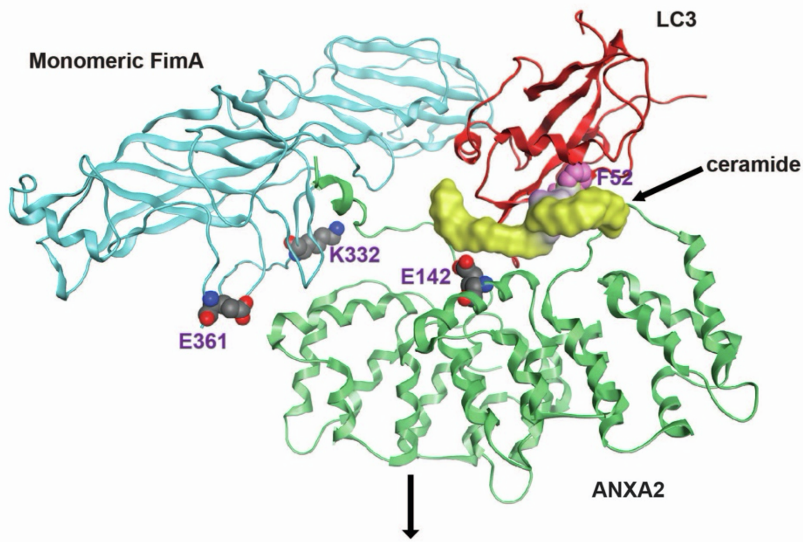

B

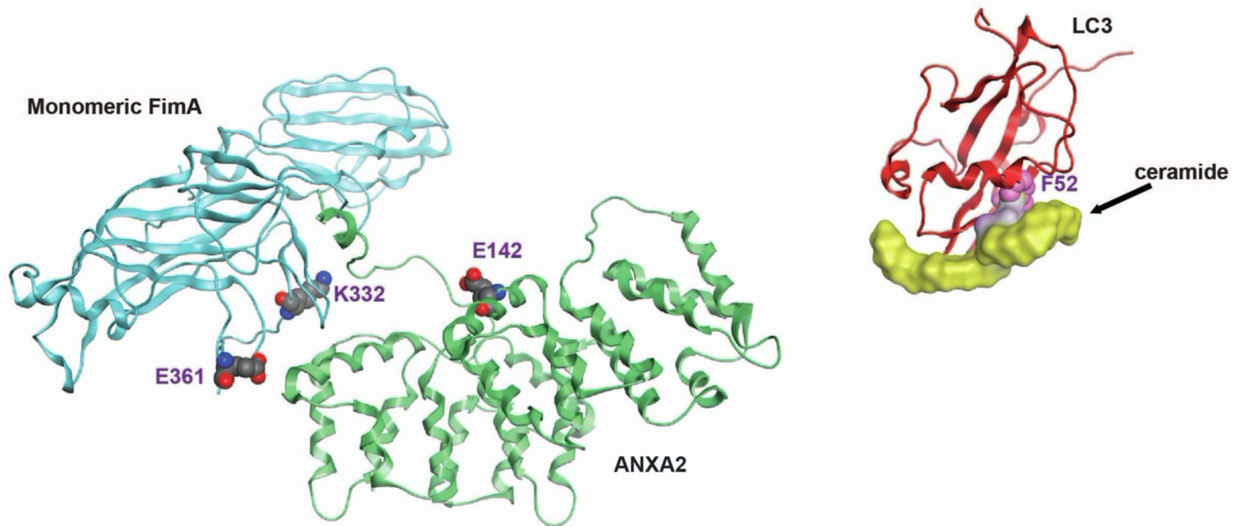

Supplemental Figure S5. ***In silico*** **modeling of monomeric FimA, ANXA2, ceramide, and LC3 in complex, Related to Figure 4. A.** Modelling of FimA-ANXA2-ceramide-LC3 complex with residues of interest shown. Monomeric FimA was projected to interact with ANXA2 at E361 and/or K332. ANXA2 was previously shown to interact with ceramide at E142, and LC3 interacts with ceramide at F52. **B.** Projected disruption of the ANXA2-ceramide-LC3 mitophagy complex by *P. gingivalis* FimA. FimA association with ANXA2 displaced ceramide and LC3, preventing mitophagy.

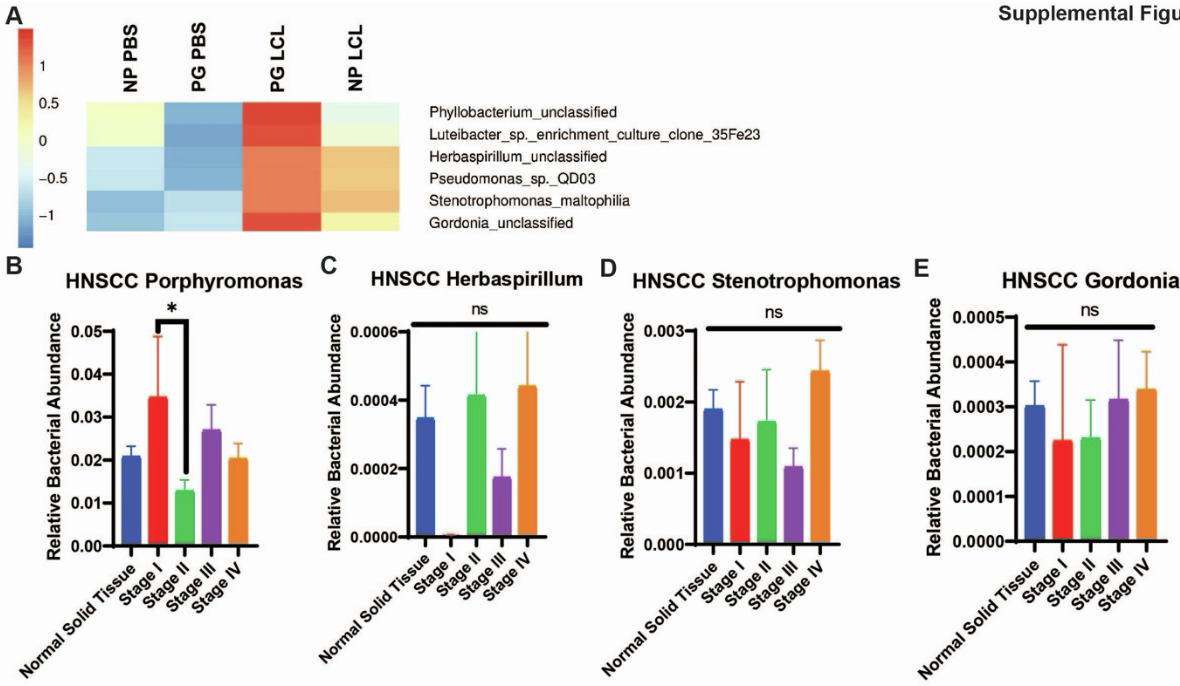
Supplemental Figure 6
A
NP PBS
PG PBS
PG LCL
NP LCL
1
0.5
0
−0.5
−1
Phyllobacterium_unclassified
Luteibacter_sp._enrichment_culture_clone_35Fe23
Herbaspirillum_unclassified
Pseudomonas_sp._QD03
Stenotrophomonas_maltophilia
Gordonia_unclassified
B
HNSCC Porphyromonas
*
Relative Bacterial Abundance
0.05
0.04
0.03
0.02
0.01
0.00
Normal Solid Tissue
Stage I
Stage II
Stage III
Stage IV
C
HNSCC Herbaspirillum
ns
0.0006
0.0004
0.0002
0.0000
D
HNSCC Stenotrophomonas
ns
0.003
0.002
0.001
0.000
E
HNSCC Gordonia
ns
0.0005
0.0004
0.0003
0.0002
0.0001
0.0000

Supplemental Figure S6. Examining the microbiome using 16S RNA sequencing, Related to Figure 6. A. Differences in the microbial composition within mouse orthotopic OSCC tumor tissue were analyzed by sequencing the prokaryotic 16S rDNA transcript via the V3-V4 hypervariable regions. Data represents species abundance (log2 fold change) in at least three independent experiments. **B.** Analysis of *Porphyromonas* abundance in human patient sample data deposited in the Bacteria in Cancer (BIC) database. *Porphyromonas* abundance was significantly higher in Stage I head and neck squamous cell carcinoma (HNSCC) than in other stages or normal control tissue. **C-E.** The abundance of alternative bacterial species *Herbaspirillum, Stenotrophomonas*, or *Gordonia*, in contrast to *Porphyromonas*, was not significant (ns). Data represents mean ± SEM analyzed via parametric t-test (n=21-568 human patient samples).